Supporting Information

Isomerization Enhanced Quantum Yield of Dibenzo[*a*,*c*]phenazine-Based Thermally Activated Delayed Fluorescence Emitters for Highly Efficient Orange OLEDs

Changjiang Zhou,[a,b] *Wen-Cheng Chen,*[c] *He Liu,*[a] *Xiaosong Cao,*[a] *Nengquan Li,*[a] *Youming Zhang,*[a] *Chun-Sing Lee,**[c] *Chuluo Yang**[a]

[a] Shenzhen Key Laboratory of Polymer Science and Technology, College of Materials Science and Engineering, Shenzhen University, Shenzhen 518060, P. R. China

[b] College of Physics and Optoelectronic Engineering, Shenzhen University, Shenzhen 518060, P. R. China

[c] Center of Super-Diamond and Advanced Films (COSDAF) and Department of Chemistry, City University of Hong Kong, Kowloon, Hong Kong SAR 999077, P. R. China

Contents

S-I Characterization and Measurements

S-II Synthesis

S- III Figures

S-I Characterization and Measurements

***General information*:** The ^{1}H NMR and ^{13}C NMR spectra were recorded on AVANCE 500 spectrometers at 298 K by utilizing $CDCl_3$ as solvents and tetramethylsilane (TMS) as a standard. The compounds were characterized by a Flash EA 1112, CHNS-O elemental analysis instrument. The matrix-assisted laser desorption/ionization time of flight mass spectrometry (MALDI-TOF-MS) mass spectra were recorded using an AXIMA-CFR^{TM} plus instrument. Thermal gravimetric analysis (TGA) was undertaken on a PerkinElmer thermal analysis system at a heating rate of 10 °C min^{-1} and a nitrogen flow rate of 80 mL min^{-1}. The temperature of degradation (T_d) was correlated to a 5% weight loss.

***Photophysical measurements*:** UV-vis absorption spectra were recorded on a UV-3100 spectrophotometer. Fluorescence measurements were carried out with a RF-5301PC. PL efficiencies in solvents and in films were respectively measured in quartz cell and on quartz plate using an integrating sphere apparatus. The room-temperature lifetimes were measured on an Edinburgh FLS-980 with an EPL-375 optical laser. The solid state absolute PLQYs were measured on a Quantaurus QY measurement system (C9920-02, Hamamatsu Photonics) equipped with a calibrated integrating sphere in the host of CBP (10 wt%) and all the samples were excited at 350 nm. During the PLQY measurements, the integrating sphere was purged with pure and dry argon to maintain an inert environment.

***Quantum chemical calculations*:** All the density functional theory (DFT) calculations were carried out using Gaussian 09 (version D.01) package on a PowerLeader cluster. The ground-state geometry was fully optimized using DFT with B3LYP hybrid functional at the basis set level of 6-31G(d, p). The excited-state properties were obtained by time-dependent density functional theory (TD-DFT) at the basis set level of PBE0/def2-SVP. The Huang-Rhys (HR) factors for $S_1 \rightarrow S_0$ transition were conducted with the DUSHIN module in MOMAP (Molecular Materials Property Prediction Package).

***Electrochemical characterization*:** Cyclic voltammetry (CV) was performed with a BAS 100W Bioanalytical Systems, using a glass carbon disk (Φ = 3 mm) as the working electrode, a platinum wire as the auxiliary electrode with a porous ceramic wick, Ag/Ag^{+} as the reference electrode, standardized for the redox couple ferricinium/ferrocene. All solutions were purged with a nitrogen stream for 10 min before measurement. The procedure was performed at room temperature and a nitrogen atmosphere was maintained over the solution during measurements.

***Device fabrication and performances*:** ITO-coated glass with a sheet resistance of 15 Ω $square^{-1}$ was used as the substrate. Before device fabrication, the ITO glass substrates were cleaned by deionized water, isopropyl alcohol, acetone and chloroform with ultrasonic cleaner. After treated with UV-zone for 30 min, ITO glasses were transferred

to a vacuum deposition system with the base pressure lower than 5 x 10^{-4} Pa for organic and metal deposition. The devices were fabricated by evaporating organic layers with an evaporation rate of 0.5-0.8 Å s^{-1}. The cathode was completed through thermal deposition of LiF at a deposition rate of 0.1 Å s^{-1}, and then capped with Al through thermal deposition at a deposition rate of 3-5 Å s^{-1}. Electroluminescence spectra and the corresponding luminance were recorded using PMA-12 photonic multichannel analyzer (Hamamatsu), and the current density-voltage-luminance characteristics were measured by computer controlled Keithley 237 power source (Tektronix) under ambient atmosphere.

***Calculation of the rate constants*:** The rate constants of excited state dynamics were calculated through following equations:

$$\Phi = \Phi_{PF} + \Phi_{TADF} \tag{4}$$

$$k_r = \Phi_{PF}/\tau_{PF} \tag{5}$$

$$\Phi = k_r/(k_r + k_{nr}) \tag{6}$$

$$\Phi_{PF} = k_r/(k_r + k_{isc} + k_{nr}) \tag{7}$$

$$k_{risc} = k_p k_d \Phi_{TADF}/k_{isc}\Phi_{PF} \tag{8}$$

$$k_p = 1/\tau_{PF} \tag{9}$$

$$k_d = 1/\tau_{TADF} \tag{10}$$

Where Φ is the quantum yield of luminescence under nitrogen atmosphere, Φ_{PF} is the quantum yield of prompt fluorescence, Φ_{TADF} is the quantum yield of delayed fluorescence, τ_{PF} is the lifetime of prompt fluorescence, τ_{TADF} is the lifetime of delayed fluorescence, k is the rate constant, and the angle standards p, d, r, nr, ISC and RISC represent the fluorescence, phosphorescence, radiative transition, non-radiative transition, intersystem crossing and reverse intersystem crossing, respectively.

S-II Synthesis

All the reagents and solvents used for the synthesis were purchased from Aldrich or Acros and used as received. All reactions were performed under nitrogen atmosphere.11-bromodibenzo[*a*,*c*]phenazine was synthetized as our previous work.

10-bromodibenzo[a, c]phenazine

A mixture of phenanthrene-9,10-dione (5 mmol) and 3-bromobenzene- 1,2-diamine (5 mmol) in acetic acid (80 mL) was heated to reflux for 8 h. After cooling to room temperature, the resulting mixture was poured into ethanol (200 mL), and then filtered. The solid was washed with ethanol several times. The crude product was purified by column chromatography on silica gel (eluent: dichloromethane) and dried under vacuum to give the desired compound as a yellow solid in 90% yield (1.62 g). 1H NMR (500 MHz, CDCl3) δ 9.48 (dd, J = 7.8, 1.4 Hz, 1H), 9.38 – 9.30 (m, 1H), 8.54 (t, J = 7.3 Hz, 2H), 8.27 (d, J = 8.5 Hz, 1H), 8.16 (dd, J = 7.4, 0.9 Hz, 1H), 7.80 (dd, J = 10.8, 4.3 Hz, 2H), 7.75 (dd, J = 12.7, 7.0 Hz, 2H), 7.71 – 7.65 (m, 1H). MALDI-TOF MS (mass m/z): 361.7 $[M(H)]^+$.

S- III Figures

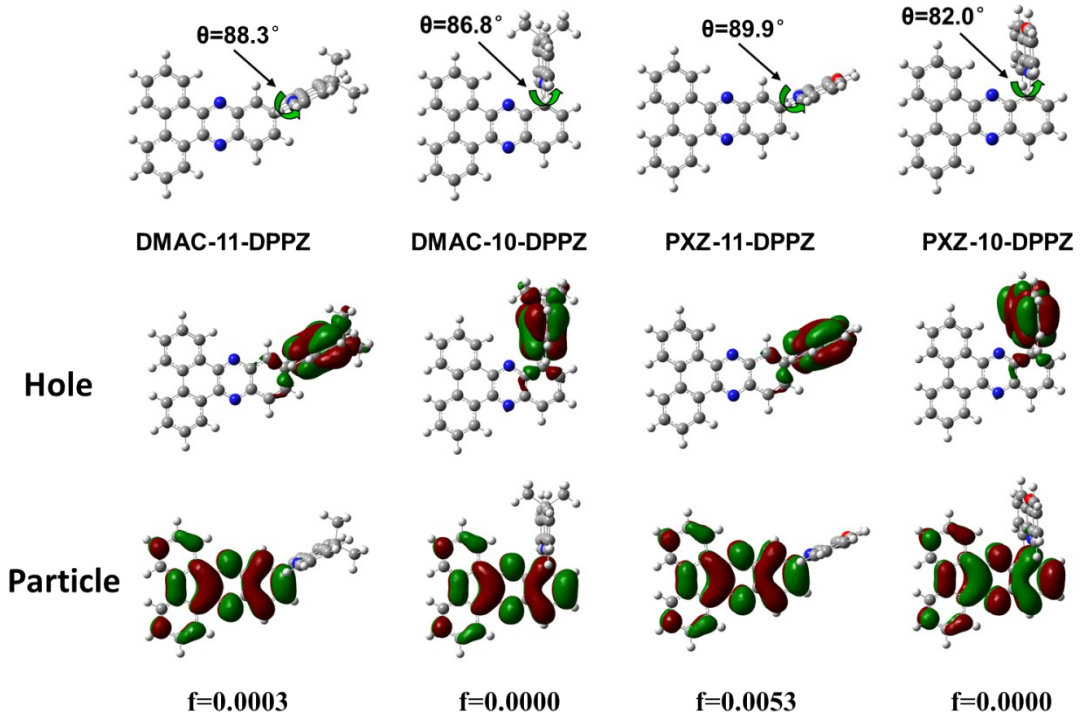

Figure S1. The optimized ground state geometries, natural transition orbital (NTO) distribution and oscillator strength of four compounds.

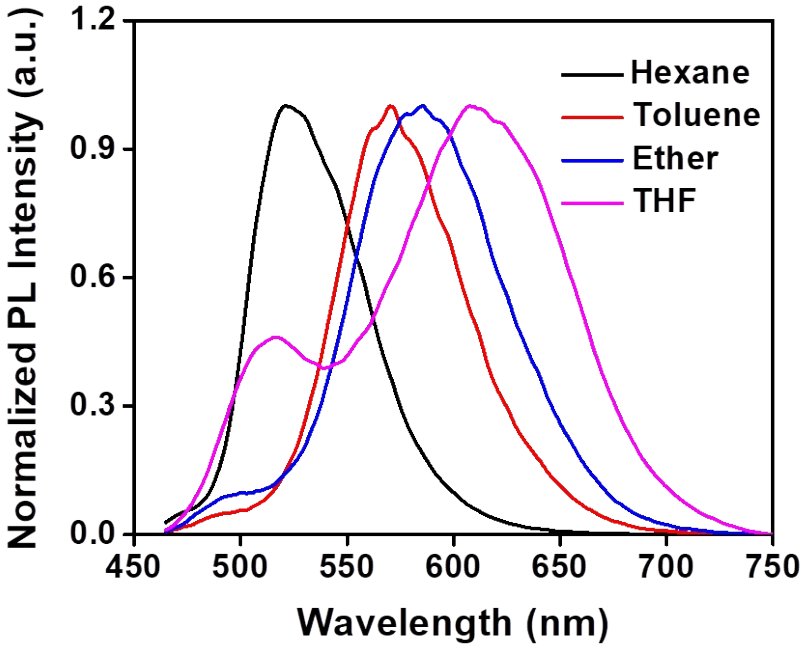

Figure S2. The solvatochromic PL spectra of DMAC-11-DPPZ.

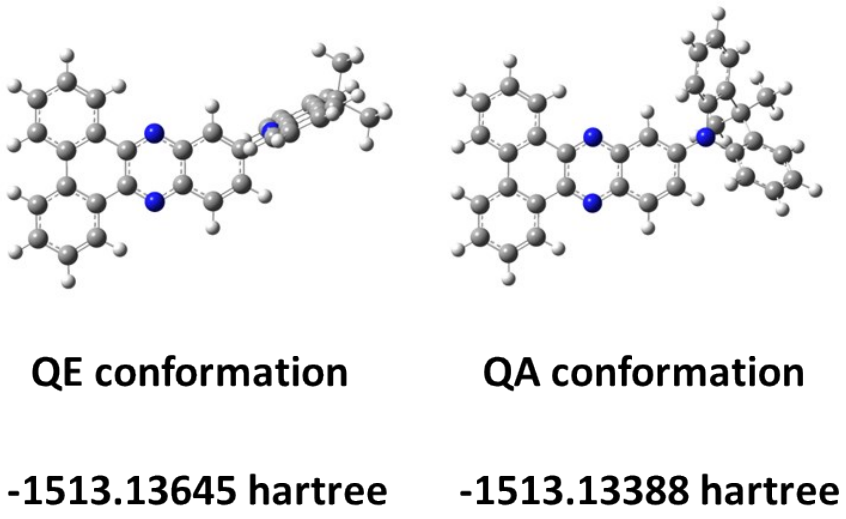

Figure S3. The optimized geometries of the quasi-equatorial (QE) and quasi-axial (QA) conformations for DMAC-11-DPPZ.

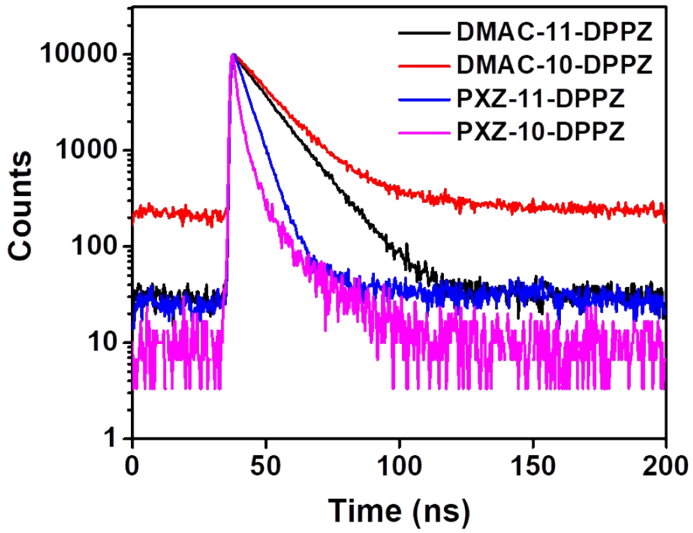

Figure S4. The transient PL spectra of prompt fluorescence for the four molecules.

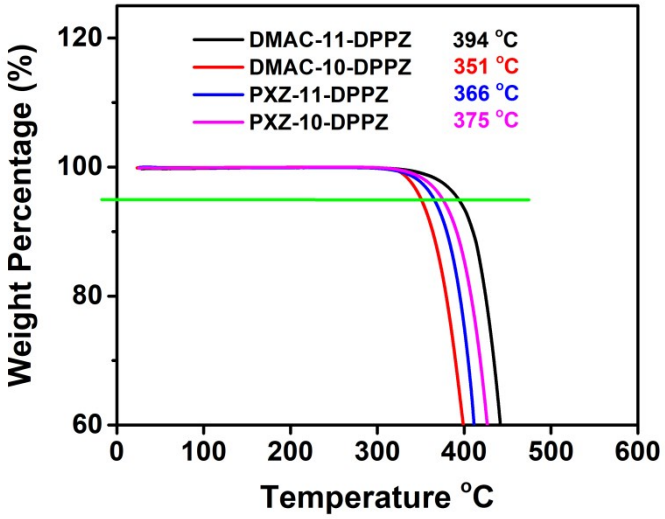

Figure S5. The thermal gravimetric analysis (TGA) curves and thermal degradation temperatures for compounds.

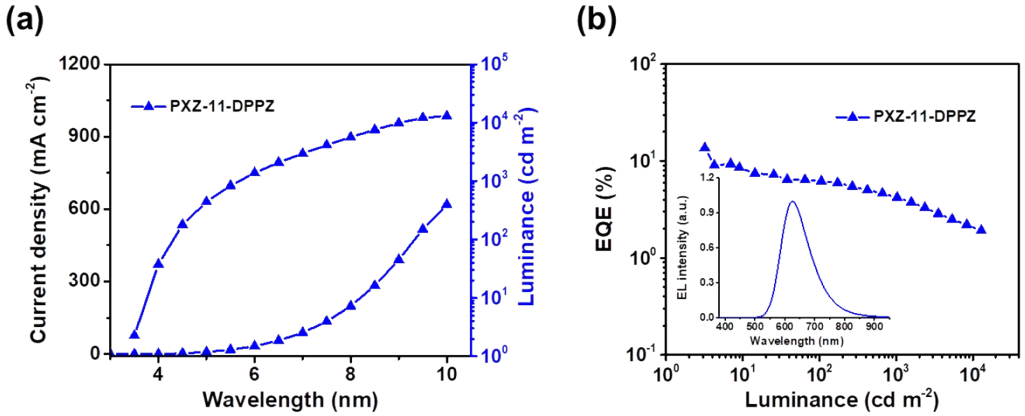

Figure S6. (a) Current density-voltage-brightness characteristics (*J*-*V*-*L* curves) and (b) EL spectrum and external quantum efficiency versus luminance curves of doped OLEDs based on PXZ-11-DPPZ.

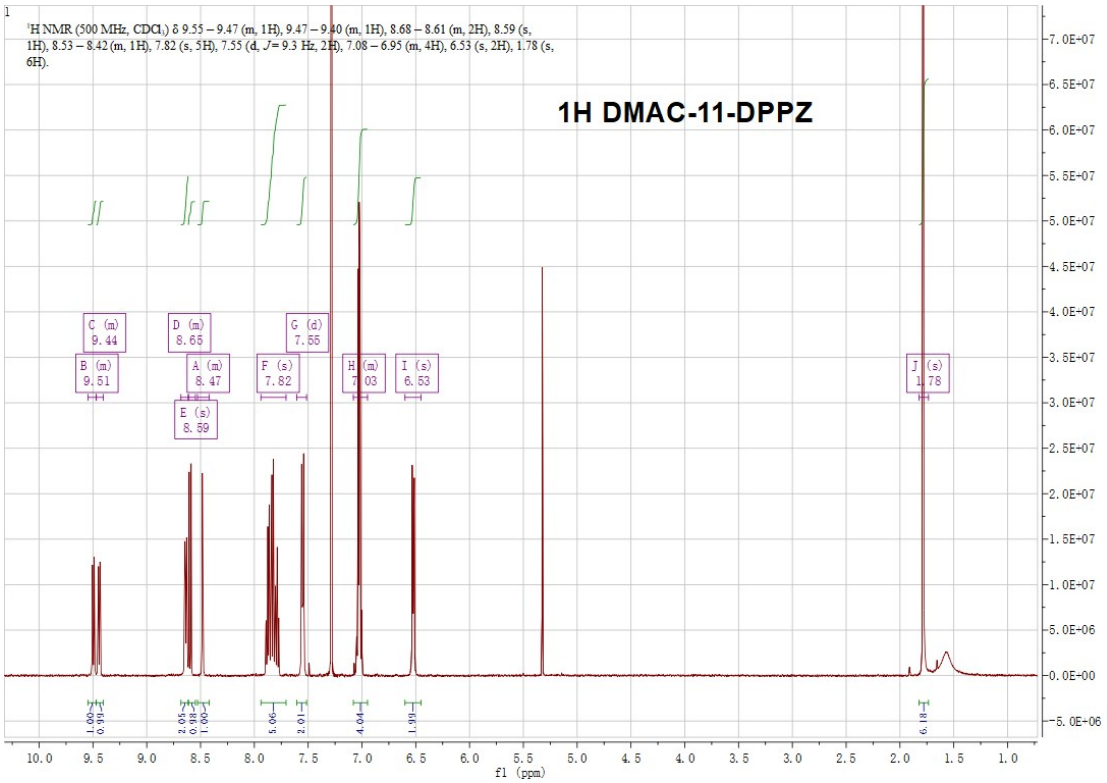

Figure S7. The ^{1}H NMR spectrum of DMAC-11-DPPZ.

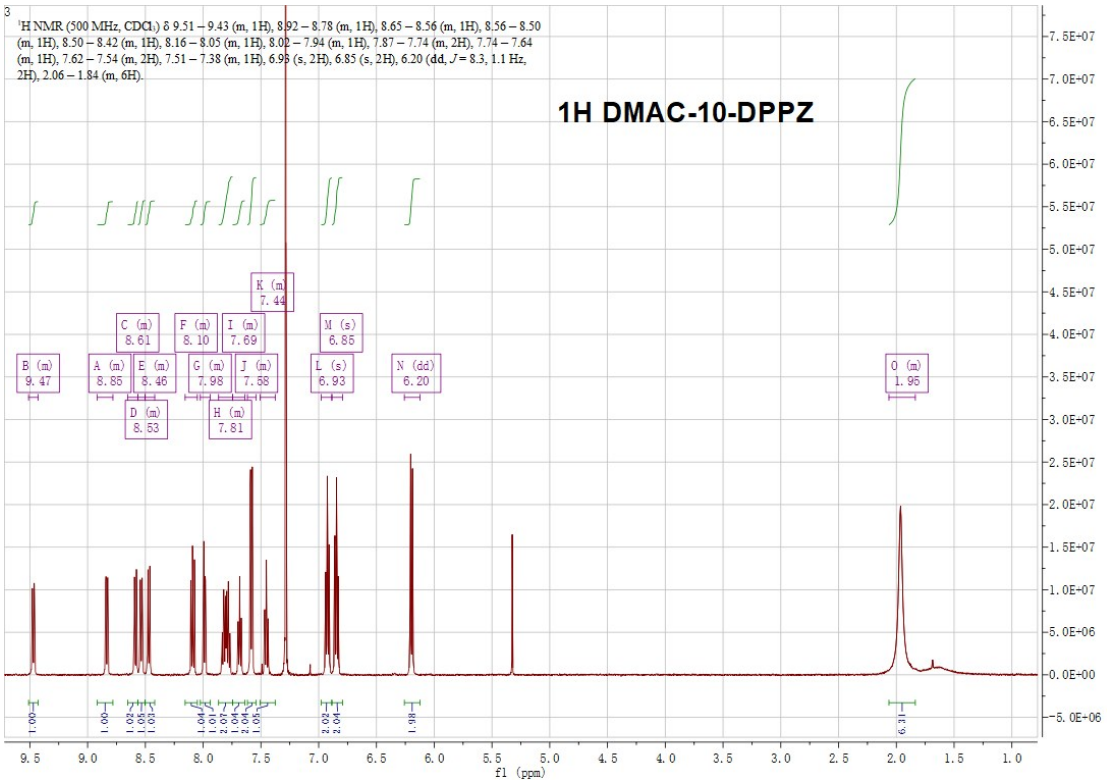

Figure S8. The ^{1}H NMR spectrum of DMAC-10-DPPZ.

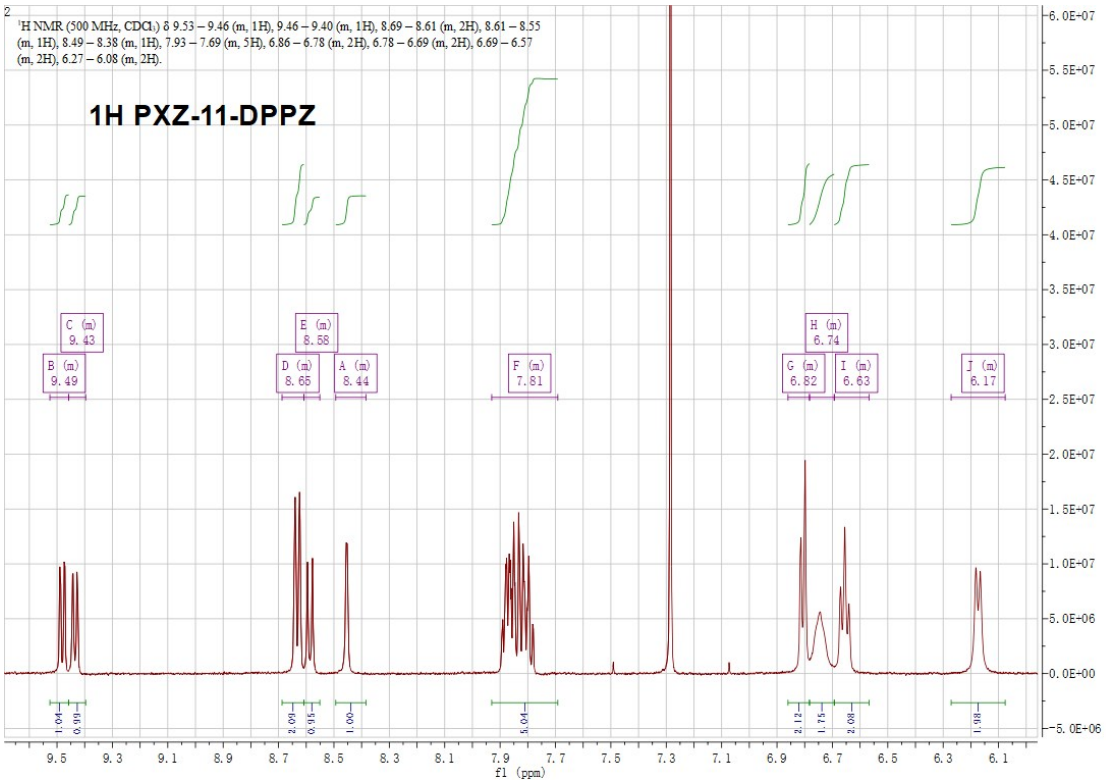

Figure S9. The ^{1}H NMR spectrum of PXZ-11-DPPZ.

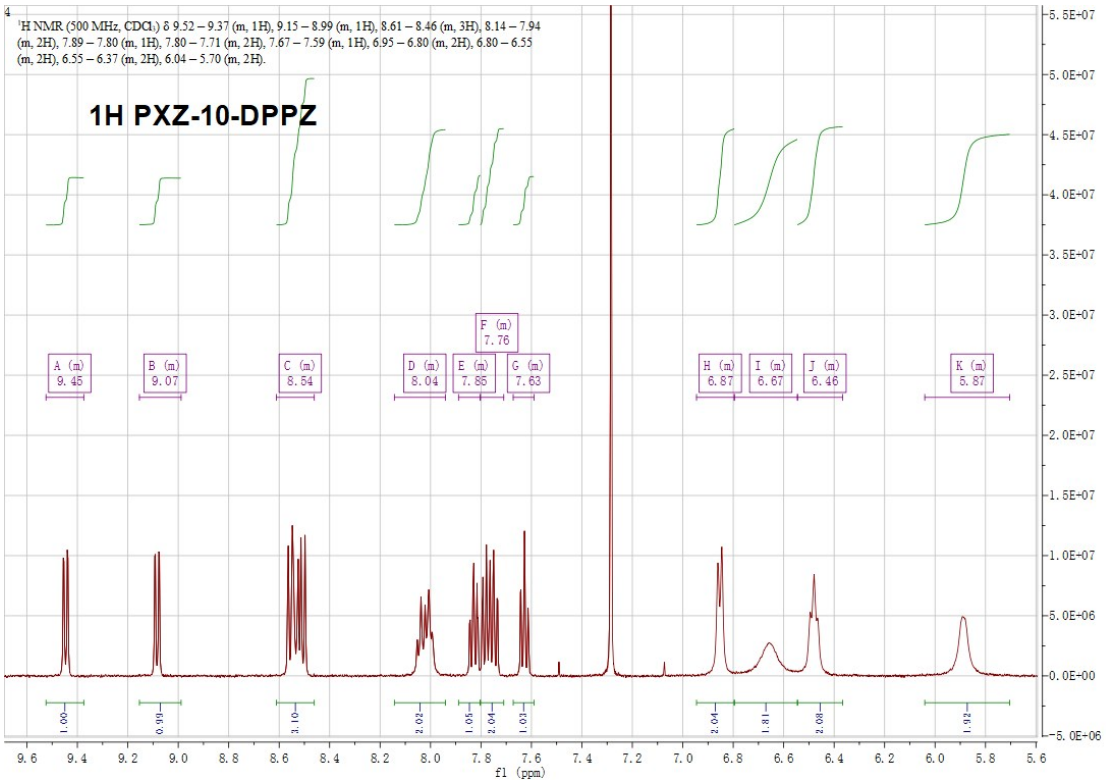

Figure S10. The ^{1}H NMR spectrum of PXZ-10-DPPZ.

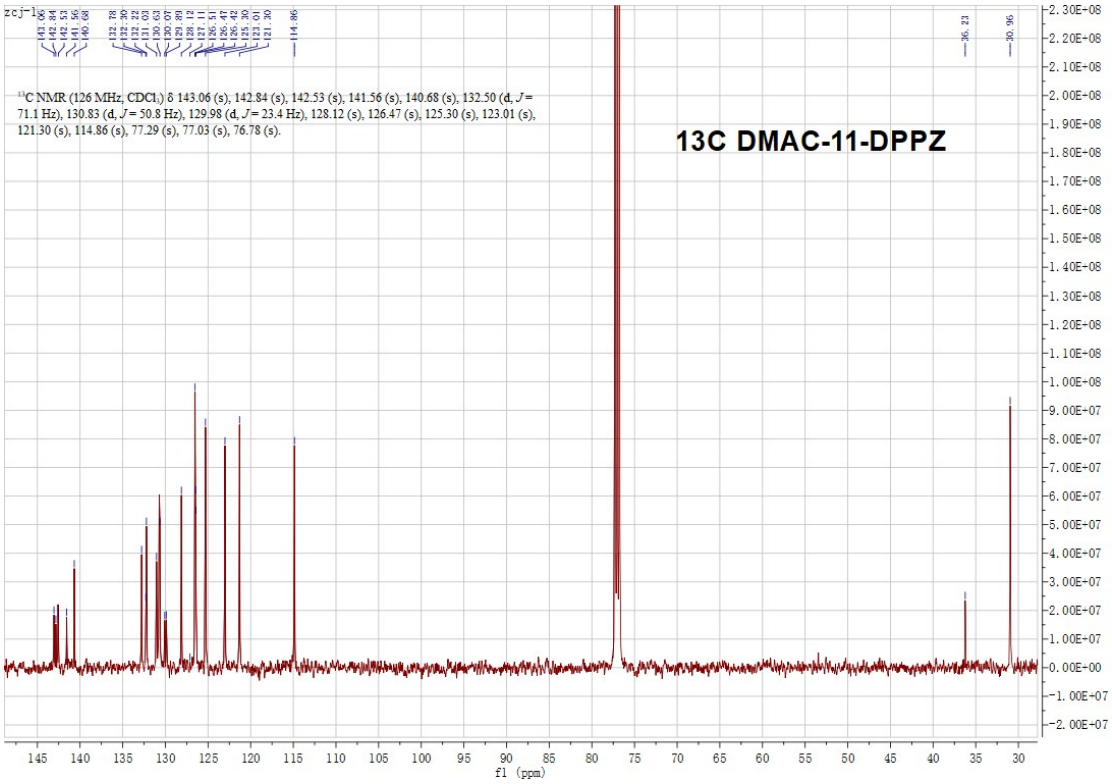

Figure S11. The ^{13}C NMR spectrum of DMAC-11-DPPZ.

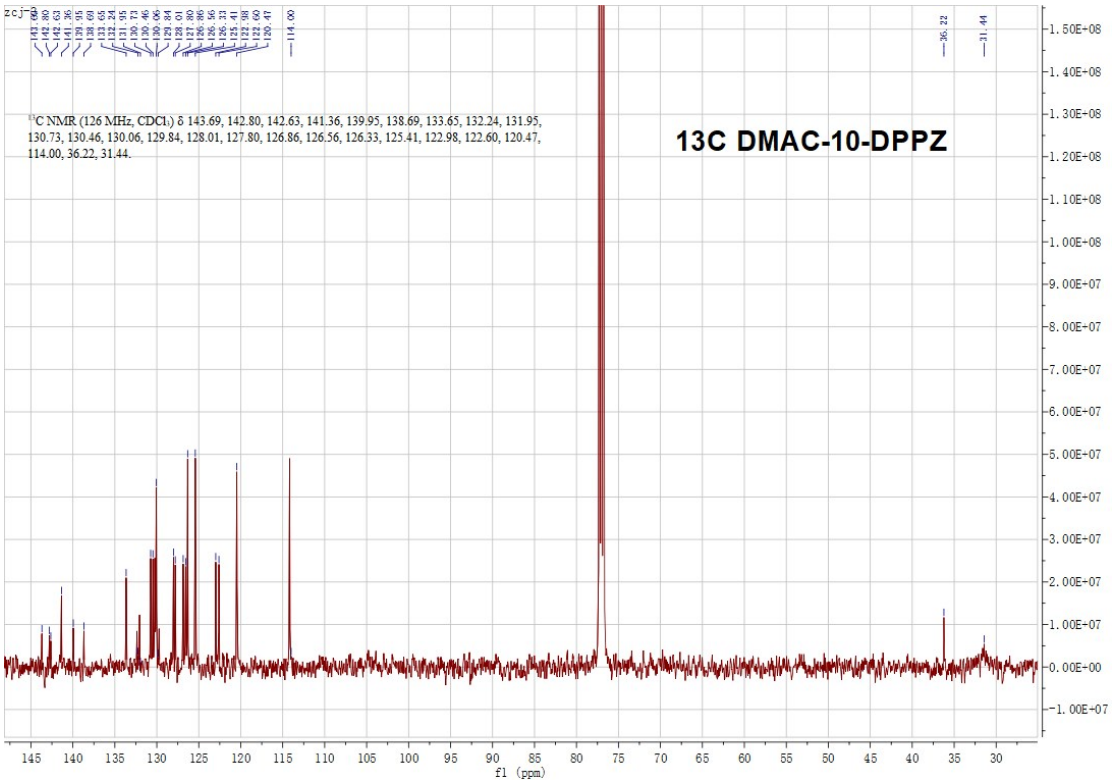

Figure S12. The ^{13}C NMR spectrum of DMAC-10-DPPZ.

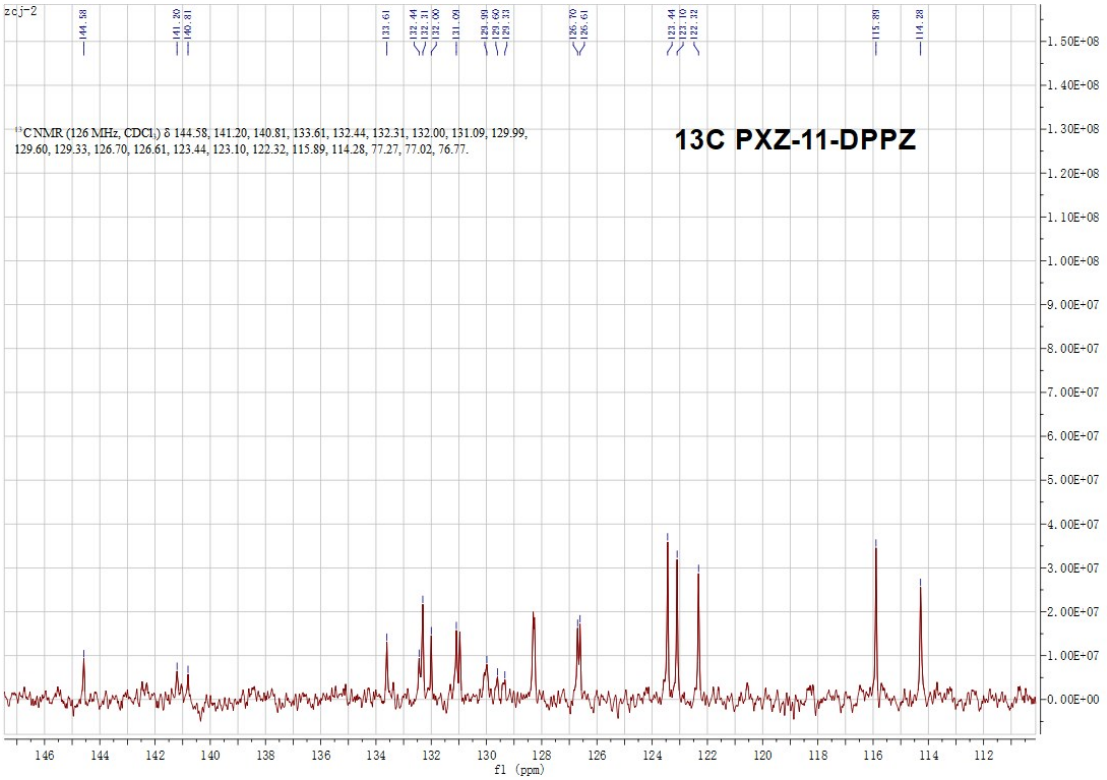

Figure S13. The ^{13}C NMR spectrum of PXZ-11-DPPZ.